Journal of Applied Polymer Science

Influence of curing sequence on phase structure and properties of bisphenol A-aniline benzoxazine/*N,N′*-(2,2,4-trimethylhexane-1,6-diyl) bis (maleimide)/imidazole blend

Zhi Wang,[1,2] Ni Cao,[1] Yu Miao,[2] Yi Gu[2]

[1]School of Materials Science and Engineering, Research Center for Engineering Technology of Polymeric Composites of Shanxi Province, North University of China, Taiyuan 030051, People's Republic of China

[2]College of Polymer Science and Engineering, State Key Laboratory of Polymeric Materials Engineering, Sichuan University, Chengdu 610065, People's Republic of China

Correspondence to: Z. Wang (E-mail: shikouri@163.com) and Y. Gu (E-mail: guyi@scu.edu.cn)

ABSTRACT: The effects of different catalysts on the curing sequences of bisphenol A-aniline benzoxazine (BA-a)/*N,N′*-(2,2,4-trimethylhexane-1,6-diyl) bis (maleimide) (TBMI) blends were studied, and the influence of curing sequences on the phase structure and properties of products was discussed. In BA-a/TBMI/adipic acid, BA-a homopolymerized first, followed by the copolymerization between TBMI and ring-opened benzoxazine. This curing sequence led to strong copolymerization, which limited the movement of components and resulted in homogeneous structures of the final products. However, in BA-a/TBMI/imidazole, TBMI homopolymerized firstly, followed by the homopolymerization of BA-a. BA-a and TBMI hardly copolymerized, and the products presented phase-separated (bi-continuous phase) structures finally. The degree of copolymerization and phase structures of products differed due to different curing sequences when different catalysts were used. Furthermore, the product with phase-separated structures had improved thermal property and toughness compared to those of the product with homogeneous structures. © 2015 Wiley Periodicals, Inc. J. Appl. Polym. Sci. **2016**, *133*, 43259.

KEYWORDS: blends; catalysts; copolymers; crosslinking; phase behavior

Received 7 August 2015; accepted 23 November 2015

DOI: 10.1002/app.43259

INTRODUCTION

Reaction-induced phase separation, which was proposed at the end of the 1980s to improve the toughness of thermoset (TS) resins,[1,2] is defined as follows. Initially, a binary homogeneous mixture forms, consisting of TS monomers and a low-molecular-weight second component. The TS monomers polymerize upon curing. At some point (cloud point) during curing, phase separation occurs following a special mechanism in the unstable region because the second component becomes increasingly immiscible with increasing polymer chain length from the thermodynamic point of view. While the mixture undergoes phase separation, the polymerization of TS monomers continues. This leads to the formation of a three-dimensional network which stops the phase separation process because of increased viscosity. The second component is composed by rubber or thermoplastic (TP) traditionally, however, the problem for rubber/TS[3,4] and TP/TS[5–10] is obvious. For rubber/TS,[11–13] the rubber component reduces T_g, modules and the resin performance in hot conditions in comparison to those of unmodified TS, even though the toughness of cured TS is elevated largely. For TP/TS, TP is inherently tough and can reduce the brittleness of TS without sacrificing their other properties significantly,[14–17] but the processability of TS deteriorates due to the high-molecular-weight TPs in the blend. Introducing phase-separated structure in TS/TS blend through reaction-induced phase separation can effectively improve the toughness property and conquer the weakness of traditional phase separation systems.[18,19] This idea is different from traditional phase separation process and also the most reported system which can form interpenetrating polymer networks (IPNs). Both components of the blend used in this idea can react to form a three-dimensional network, whereas only one in the traditional reaction-induced phase separation system can do so. Therefore, controlling the morphology and understanding the mechanism of reaction-induced phase separation in TS/TS blend are rather complicated. On the other hand, most IPNs have a nanoscale phase-separated structure which is typified by an unobvious phase-separated structure (close to the homogeneous structure) and only one peak in the Tan Delta curve.[20,21] The beneficial

effect of this structure (nanoscale phase-separated structure) on the toughness of TS/TS blend has not been reported hitherto. Thus, compared with IPNs, introducing phase-separated structure in TS/TS blend means that the size of this structure should reach the micrometer range which has a positive effect on the toughness property.

Different from the traditional reaction-induced phase separation system, in the TS/TS system, the control of relative reaction rate, and the curing sequences of two components are crucial for the phase-separated structure and properties.[22] The relative reaction rate of two components has been controlled by changing the initial curing temperature in a previous work.[23] However, there remain no studies on the control of the curing sequences of two components in the TS/TS system, even though this factor has been discussed thoroughly in the system with IPNs.

The curing sequence of two components which can form IPNs has an influence on the final structure.[24–27] Decker *et al.*[24] used radical- and cationic-type photoinitiators to catalyze the reaction of a mixture of acrylate and epoxide monomers, and found that the polymerization of acrylate proceeded faster than the cationic polymerization of epoxide. The whole system formed fully cured IPNs. However, after the blend was put in the air, epoxide polymerized faster than acrylate did, and the blend formed incompletely cured IPNs within seconds. Yang *et al.*[25] investigated the effect of changing curing sequence on an acrylate/urethane IPN through photochemical initiation of acrylate and thermal polymerization of urethane. When urethane reacted prior to acrylate did, a homogeneous IPN was obtained. However, if acrylate polymerized first, a phase-separated structure was obtained. Dean *et al.*[26] studied the influence of curing sequence of imidazole-cured epoxy and different azo initiators-polymerized dimethacrylate on IPNs. When dimethacrylate was cured faster than epoxy, fully cured IPNs formed. If epoxy polymerized first, incompletely cured IPNs formed. The different IPNs led to different thermal properties. As shown above, the final structure of IPNs is determined by the used catalyst, and different catalysts can cure the components according to the mechanisms and curing sequences of two components in the blend. In conclusion, the final structure of IPNs can be effectively and simply adjusted by changing the curing sequence. However, whether curing sequence can modulate the phase-separated structure in TS/TS blend based on reaction-induce phase separation is still unknown. Hence, evaluating the influence of curing sequence of two components on introducing an obvious phase-separated structure (not IPN structure) in TS/TS blend through reaction-induced phase separation may help control the morphology conveniently. However, it is not suitable to introduce two or more kinds of catalysts like the IPNs systems reported previously, because catalysts may undermine the properties of TS/TS blends.[28] Instead, studies involving only one kind of catalyst are preferred.

Bisphenol A-aniline benzoxazine (BA-a) and *N,N′*-(2,2,4-trimethylhexane-1,6-diyl) bis (maleimide) (TBMI) were used in this study. Four different kinds of catalysts, which belong to two categories, were chosen. The effects of different catalysts on the reaction of two components were discussed. The different curing sequences by using different catalysts were observed and their influence on phase structures was discussed. Furthermore, the influence of phase-separated structure on toughness and thermal property was discussed, and such structured product enjoyed improved properties.

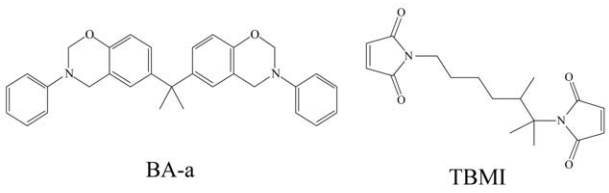

Scheme 1. The structure of BA-a and TBMI.

EXPERIMENTAL

Materials

Bisphenol A-aniline benzoxazie monomer (BA-a, mp 113°C) was synthesized and purified according to procedures preciously described.[29] *N,N′*-(2,2,4-trimethylhexane-1,6-diyl) bis (maleimide) (TBMI, mp 88°C) was synthesized and purified in our laboratory following the reported procedure.[30] The structure of BA-a and TBMI is shown in Scheme 1.

Bisphenol A, aniline, aqueous formaldehyde solution, imidazole (I), diethyl tetramethyl imidazole (D), oxalic acid (O), adipic acid (A), toluene, acetone, maleic anhydride, and ethyl alcohol were provided by Chengdu Kelong Chemical Reagents (China). Toluene sulfonic acid was supplied by Shanghai QianFeng Chemical (China). Trimethylhexamethylenediamine was purchased from Shanghai BaoMan biotechnology (China).

Preparation of the Blend Sample

BA-a was blended with TBMI in a mole ratio of 1/1 (BA-a/TBMI) at 110°C for 10 min and subsequently cooled to 25°C. Then, imidazole, diethyl tetramethyl imidazole, oxalic acid, and adipic acid with 3 wt % of blend dissolved in acetone were added into the blend respectively and stirred for 10 min. The blends of BA-a/TBMI with imidazole, diethyl tetramethyl imidazole, oxalic acid, and adipic acid were defined as BTI113, BTD113, BTO113, and BTA113, respectively. Besides, the BTI213 and BTI123 (mole ratio of BA-a to TBMI is 2/1 and 1/2, respectively) were prepared as above. The monomer mixed with catalyst followed the same procedure and the amount of catalyst was 3 wt % of monomer also. After that, different systems were cast into an aluminum plate and degassed under vacuum at 60°C for 1 h, and then transferred to a metal mold. The casts were cured with a profile as following: 120°C/4 h, 160°C/4 h, and 200°C/2 h.

Measurements

Curing behavior was studied by differential scanning calorimetry (DSC) and Fourier transform-infrared spectroscopy (FT-IR), which were performed on TA Instrument DSC-Q20 and Nicolet 5700 FT-IR spectrometer, respectively. The non-isothermal tests for BTI113 were conducted at a heating rate of 10°C min^{-1}. The heating rate of 5, 10, 15, and 20°C min^{-1} was used to find the peak temperatures of different blends under different heating rate. The Kissinger method[31] was used when calculated the

Table I. Activation Energies for Polymerization of Different Components with Different Catalysts

Catalyst	Imidazole	Diethyl tetramethyl imidazole	Oxalic acid	Adipic acid	Without catalyst
BA-a (Ea (kJ mol^{-1}))	71.17	93.77	61.80	66.95	95.61
TBMI (Ea (kJ mol^{-1}))	44.06	87.90	113.9	221.2	89.73

activation energy for polymerization. The original Kigginger's relation is

$$\frac{d\ln\left(\frac{T_p^2}{\alpha}\right)}{d\left(\frac{1}{T_p}\right)} = E_a/R \quad (1)$$

where α is the heating rate, T_p is the peak temperature, and R is the gas constant. All tests of DSC were under a nitrogen flow rate of 50 mL min^{-1}. FT-IR spectrum of the sample was taken using the KBr pellet with a resolution of 4 cm^{-1} and a scanning time of 32 times.

The morphology of the cured sample was observed by field emission-scanning electron microscope (FESEM) FEI Inspect F. The samples were fractured in liquid nitrogen. Then the fractured surfaces were coated with gold and observed with accelerating voltage of 20 KV.

The phase morphology of the cured blend was also investigated by transmission electron microscopy (TEM) using a JSM-7500F apparatus. The sample was microtomed at room temperature with a Leica EMFCS instrument equipped with a diamond knife. The resulting ultrathin section of 100 nm thickness was picked up on copper grid to observe phase morphology with an accelerating voltage of 80 KV.

The thermal properties of the cured casts were obtained by using TA instruments DMA Q800 dynamic mechanical analyzer (DMA) with the sample dimension of 30 mm × 10 mm × 3 mm in three point bend mode from 40 to 370°C with a heating rate of 5°C min^{-1} and frequency of 1 Hz.

Charpy impact tests of unnotched cast specimens were carried out using a pendulum-type testing machine (XJJD-5, Jinjian, China) in accordance to GB/T2571-1995. The dimensions of sample are 80 mm × 10 mm × 4 mm (length × width × thickness). Five specimens were tested to obtain an average. The test was performed with pendulum of 2 J with a velocity of 2.9 m s^{-1}.

Bending deflection of cast specimens were carried out by a 3-point bending testing using Instron 4320. Five sets of flexural specimens with a dimension of 120 mm × 10 mm × 4 mm (length × width × thickness) were tested to obtain an average. A span of 64 mm giving a span/thickness ratio of 16 according to GB/T2570-1995 was used in the flexural test. The test was performed with a crosshead speed of 0.2 mm min^{-1}.

RESULTS AND DISCUSSION

Catalyzing Effects of Different Catalysts

To investigate the catalyzing effects of different catalysts on the reaction of BA-a and TBMI, the activation energies for polymerization of different components were calculated by the Kissinger method[31] based on the nonisothermal DSC test (Table I), and those of two components without catalyst were also shown for comparison. All four kinds of catalysts decreased the activation energy for polymerization of BA-a, meaning that BA-a reacted more easily in the presence of catalyst than pure BA-a did. For TBMI, only imidazole (I) and diethyl tetramethyl imidazole (D) managed to reduce the activation energy for polymerization to 44.06 and 87.90 kJ mol^{-1}, respectively. Oxalic acid (O) and adipic acid (A), however, increased the activation energy to 113.9 and 221.2 kJ mol^{-1}, respectively. Thus, compared with the reaction of pure TBMI, I and D showed promoting effects whereas O and A had inhibitory effects. The activation energies for polymerization of BA-a/I and BA-a/D were larger than those of TBMI/I and TBMI/D. On the other hand, the activation energies for polymerization of BA-a/O and BA-a/A were smaller than those of TBMI/O and TBMI/A, respectively. Therefore, TBMI reacted first in BTI113 and BTD113, while BA-a did so in BTO113 and BTA113. Furthermore, the difference between BA-a/I and TBMI/I exceeded that between BA-a/D and TBMI/D, and the difference between BA-a/A and TBMI/A surpassed that between BA-a/O and TBMI/O, so the discrepancy of curing reaction rate between two components was large in BTI113 and BTA113. To clarify the effect of curing sequence on the final phase-separated structure, BTI113 and BTA113 were chosen in the following study.

Curing Behaviors of BTA113 and BTI113 Studied by DSC

The curing behavior of BTA113 was studied first by DSC (Figure 1). As shown in Figure 1(a), there is a single exothermic peak centered at 217°C for BA-a/3 wt % A, with the onset

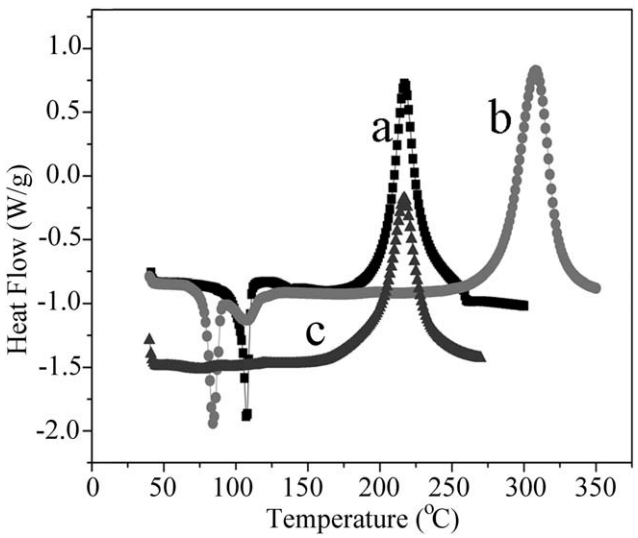

Figure 1. DSC curves of samples (a) BA-a/3 wt % A; (b) TBMI/3 wt % A; (c) BTA113.

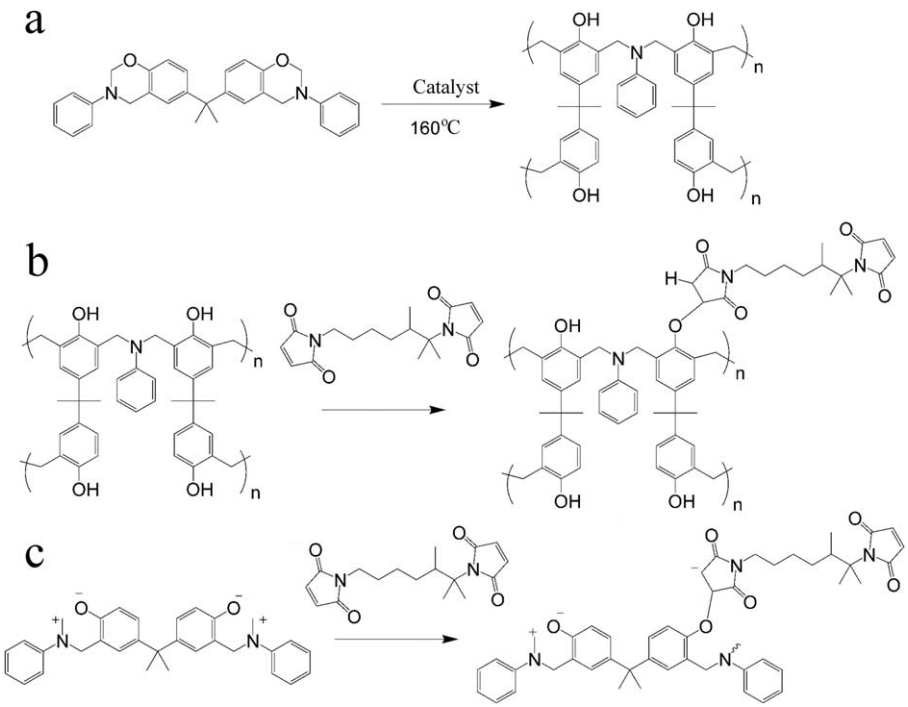

Scheme 2. (a) BA-a catalyzed by A; (b) the copolymerization between –OH and TBMI; (c) TBMI catalyzed by the $–O^-$.

temperature and enthalpy of 170°C and 170.1 kJ mol^{-1}, respectively. Compared with the onset temperature (243°C) and peak temperature (262°C)[32] of pure BA-a, A allowed BA-a to react at a lower temperature, exerting an obvious catalyzing effect. However, the onset and maximum temperatures of the exothermic peak for TBMI/3 wt % A were 250 and 308°C, respectively [Figure 1(b)]. The enthalpy of TBMI/3 wt % A was 154.4 kJ mol^{-1}. Different from BA-a/3 wt % A, A caused the curing temperature of TBMI to shift to a higher temperature compared with that of pure TBMI which had the onset and peak temperatures of 184 and 267°C, respectively.[32] Accordingly, A restrained the reaction of TBMI. These results are consistent with those of activation energy. In Figure 1(c), BTA113 exhibits a single exothermic peak with the onset temperature of 168°C and the peak temperature of 217°C. The enthalpy of BTA113 was 139.8 kJ mol^{-1}. TBMI reacted at lower temperature than TBMI/3 wt % A did. If two components only undergo self-polymerization but not copolymerization, the theoretical enthalpy of BTA113 should be 162.3 kJ mol^{-1}. Given the lower actual enthalpy (139.8 kJ mol^{-1}), TBMI underwent other types of catalytic reactions besides the polymerization of BA-a in BTA113.

Takeichi *et al.*[33] studied the copolymerization behavior of a mixture of 3-phenyl-3,4-dihydro-2H-1,3-benzoxazine (P-ABz) and 4-hydroxyphenylmaleimide, and found ether bonding. Meanwhile, since the peak temperature of P-ABz was 222°C, its purity was also not high. Gu *et al.*[32] studied the curing reaction of BA-a/TBMI blend, and found that amine group and $—O^-$ from partially opened oxazine ring effectively catalyzed the reaction of TBMI. They were subjected to copolymerization, also forming ether bonding.

The curing sequence of BTA113 was herein proposed[34] (Scheme 2) by combining previous studies with the results from Figure 1. BA-a reacted first [Scheme 2(a)], followed by the reaction of opened oxazine ring with TBMI and $—O^-$-catalyzed polymerization of TBMI at same time [Scheme 2(b,c)]. These reactions occurred within the same range of temperature as shown in Figure 1(c).

Different from adipic acid, the onset temperature of BA-a by using imidazole as catalyst was 150°C, with the peak temperature and enthalpy of 198°C and 167.7 kJ mol^{-1}, respectively [Figure 2(a)]. Meanwhile, TBMI/3 wt % I had the onset temperature of 100°C, the peak temperature of 210°C [Figure 2(b)], and the enthalpy of 133.6 kJ mol^{-1}. Compared with pure monomers, imidazole effectively catalyzed the reaction of both

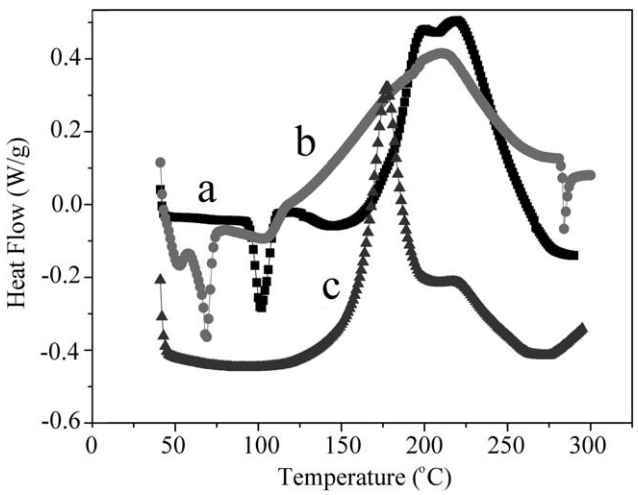

Figure 2. DSC curves of samples (a) BA-a/3 wt % I; (b) TBMI/3 wt % I; (c) BTI113.

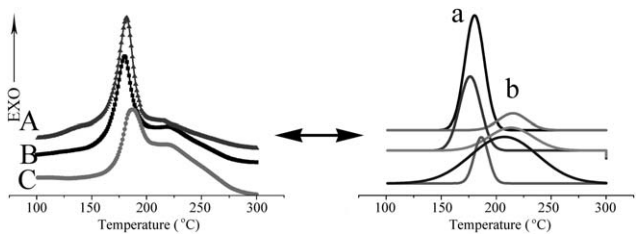

Figure 3. DSC curves of different blends and corresponding curves after Gaussian fitting (a) BTI123; (b) BTI113; (c) BTI213.

components. BTI113 had the onset temperature of 100°C, followed by the two peak temperatures at 180 and 220°C, respectively. The enthalpy of BTI113 was 149.8 kJ mol^{-1}. If there is only self-polymerization, the enthalpy should be 150.7 kJ mol^{-1} that is close to the actual one, so the two components hardly copolymerized.

To clarify the curing reaction of each peak in the DSC curve of BTI113, blends with different mole ratios (BTI213, BTI113, and BTI123) were prepared and tested (Figure 3). The area of each peak (Table II) was calculated based on the Gaussian fitting method. With decreasing amount of TBMI in blends, the height and area of peak a decreased and those of peak b increased, suggesting that the two peaks mainly corresponded to the reactions of TBMI and BA-a, respectively. As a result, the curing sequence of BTI113 was proposed (Scheme 3). TBMI reacted first [Scheme 3(a)], followed by the reaction of BA-a [Scheme 3(b)]. Because considerable TBMI had been consumed at the initial curing stage, the two components seldom copolymerized [Scheme 3(c)].

Curing Behaviors of BTA113 and BTI113 Studied by FTIR

The curing processes of BTA113 and BTI113 were monitored by FTIR to further confirm their curing sequences (Figures 4 and 5). Figures 4(A) and 5(A) exhibit bands at 943 cm^{-1} for the oxazine ring, at 1237 cm^{-1} for C—O—C of benzoxazine, at 1500 cm^{-1} for tri-substituted benzene and at 3098 cm^{-1} for =C—H of TBMI. The band at 1187 cm^{-1} for C—O—C of copolymerized structure[33] was used to monitor the copolymerization between BA-a and TBMI.

Table II. The Area of Peaks after Gaussian Fitting

	Peak a (area)	Peak b (area)
BTI123	34.1	7.2
BTI113	23.9	15.4
BTI213	10.2	47.9

In BTA113 (Figure 4), the intensities of bands at 943, 1237, 1500, and 3098 cm^{-1} remained unchanged after the sample was cured at 120°C [Figure 4(B)], indicating that the two components did not react. With increasing curing temperature (160°C), the intensities of bands at 943, 1237, and 1500 cm^{-1} decreased, while the band at 1480 cm^{-1} for tetra-substituted benzene appeared [Figure 4(C)]. Therefore, BA-a reacted at this temperature. As suggested by the simultaneously decreased intensity of band at 3098 cm^{-1}, TBMI also reacted. After the sample was cured at 200°C for 2 h [Figure 4(D)], the bands at 943, 1237, 1500, and 3098 cm^{-1} vanished, indicating that BA-a and TBMI had been consumed all. Besides, the intensity of band 1187 cm^{-1} for C—O—C of copolymerized structure between BA-a and TBMI increased with decreasing intensity of band at 3098 cm^{-1}, so the two components underwent copolymerization. The curing sequence was the same as that shown in Scheme 2 and the initial curing temperature was 160°C.

Different from BTA113, the intensity of band at 3098 cm^{-1} in BTI113 decreased at 120°C [Figure 5(B)]. However, the

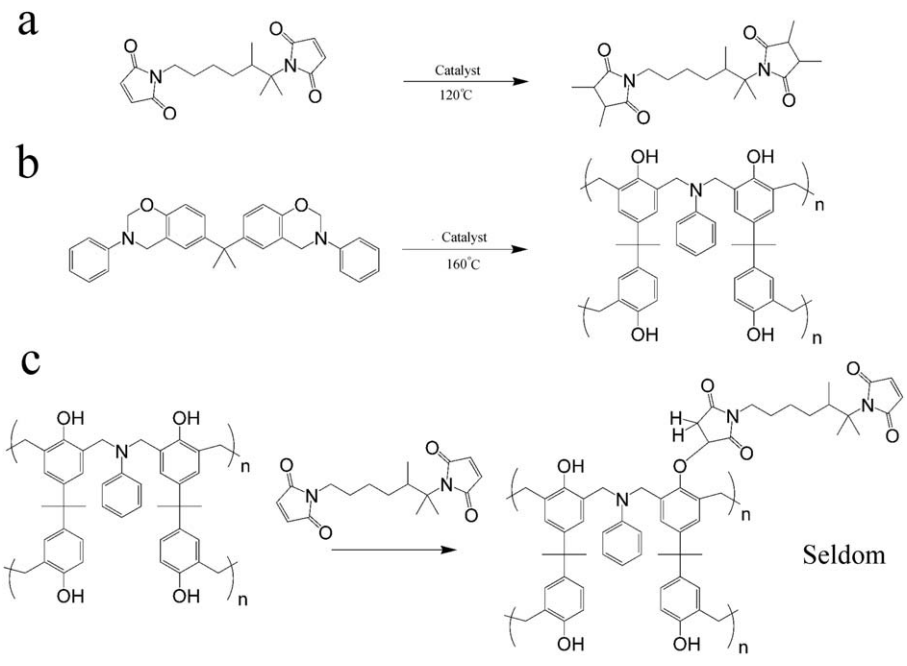

Scheme 3. (a) TBMI catalyzed by I; (b) BA-a catalyzed by I; (c) copolymerization between opened benzoxazine and TBMI (seldom).

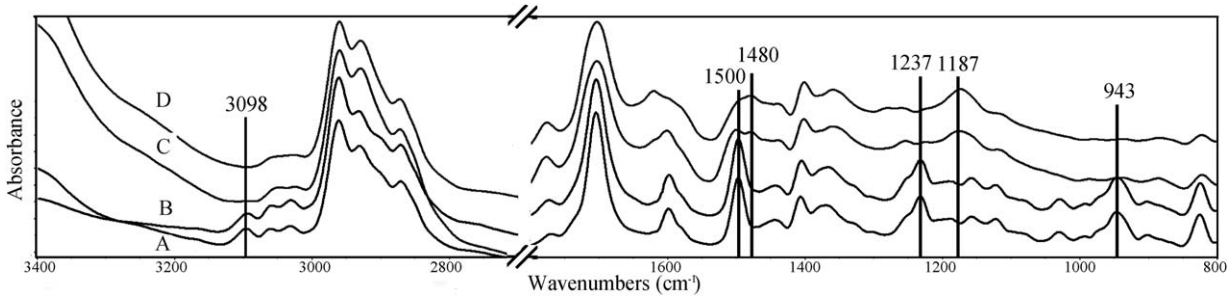

Figure 4. FT-IR spectra of BTA113 at room temperature (A) and after cure at 120°C/4 h (B); 120°C/4 h, 160°C/4 h (C); 120°C/4 h, 160°C/4 h, 200°C/2 h (D).

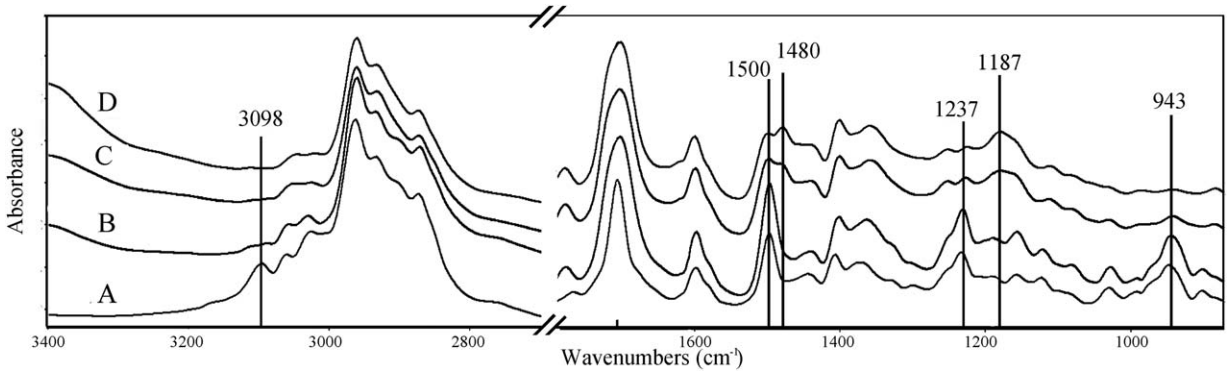

Figure 5. FT-IR spectra of BTI113 at room temperature (A) and after cure at 120°C/4 h (B); 120°C/4 h, 160°C/4 h (C); 120°C/4 h, 160°C/4 h, 200°C/2 h (D).

intensities of bands at 943, 1237, and 1500 cm^{-1} barely changed. TBMI in BTI113 reacted at 120°C at which, however, BA-a remained unreacted. When the curing temperature was increased to 160°C [Figure 5(C)], the intensity of band at 3098 cm^{-1} decreased continuously. The absorptions at 943, 1237, and 1500 cm^{-1} decreased at this temperature, accompanied by the emergence of a band at 1480 cm^{-1}, i.e. BA-a started to react at 160°C. After curing at 200°C for 2 h, the absorptions at 943, 1237, 1500, and 3098 cm^{-1} disappeared, so BTI113 was cured completely in this cycle. Furthermore, since absorption at 1187 cm^{-1} was scarce during the whole process, BA-a and TBMI hardly copolymerized. In conclusion, the curing sequence of BTI113 is shown as Scheme 3. TBMI reacted first at 120°C, and then BA-a reacted at 160°C, without undergoing copolymerization.

Influence of Curing Sequence on Phase-separated Structure

Different curing sequences can be realized by using different catalysts, the influence of which on phase-separated structure should be considered. Figure 6 shows the FESEM images of the fracture surfaces of cured BTA113 and BTI113. The fracture surface of cured BTA113 was smooth, without obvious phase-separated structure. However, the fracture surface of cured BTI113 was rough and wrinkled with strong microscopic heterogeneity, so phase-separated structure existed only in BTI113. TEM was conducted to further confirm the phase-separated structure (Figure 7). BTA113 had no phase-separated structure, as evidenced by the homogeneous structure [Figure 7(A)]. In contrast, a bi-continuous phase structure was discerned in BTI113 [Figure 7(B)]. The dark areas were attributed to PBA-a while the light areas were attributed to PTBMI, based on the higher electron density of PBA-a calculated by the structure and density of the components. From the results of FESEM and TEM, curing sequence may determine the final phase-separated structure. A homogeneous structure was obtained if BA-a reacted first, while a bi-continuous structure formed if TBMI reacted first.

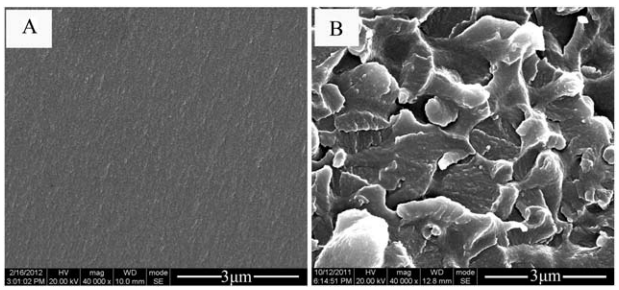

Figure 6. FESEM images of fracture surface of cured BTA113 (A) and BTI113 (B).

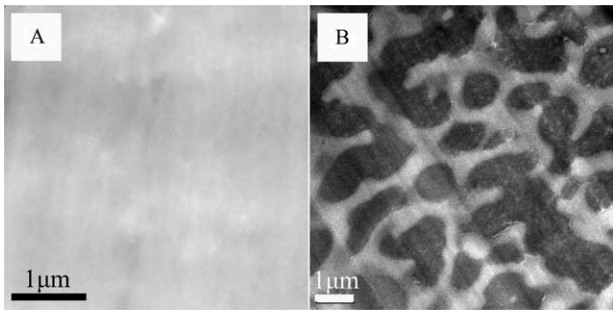

Figure 7. TEM images of cured BTA113 (A) and BTI113 (B).

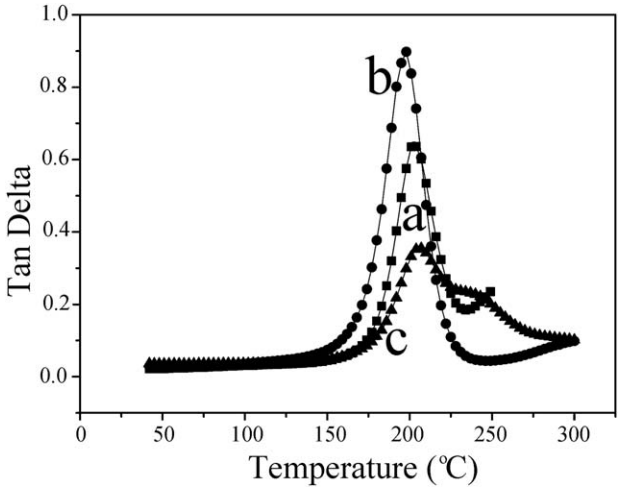

Figure 8. Tan δ curves of PBA-a (A), cured BTA113 (B) and cured BTI113 (C).

DMA is an effective method that examines different components of a multiphase system and their interactions. To further examine the phase-separated structure, DMA was performed and the tan δ curves are shown in Figure 8. The glass transition temperature T_g, defined as the temperature corresponding to the peak of tan δ in the glass transition, was 203°C for BA-a/3 wt % I [Figure 8(a)]. The tan δ curve of BTA113 had a single peak [Figure 8(b)], excluding the possibility of having a phase-separated structure. Having large amounts of C—O—C structures, BTA113 had a lower T_g (197°C) than that of BA-a/3 wt % I. However, as suggested by the two peaks in the tan δ curve [Figure 8(c)], BTI113 had a phase-separated structure. T_g of 207°C, which was close to that of PBA-a, corresponded to the rich phase of PBA-a. T_g of 239°C corresponded to the relaxation of PTBMI, even though the temperature was lower than that of PTBMI, probably because PTBMI contained BA-a. Notably, both T_g values were higher than that of BA-a/3 wt % I. Hence, the thermal property of BTI113 with a phase-separated structure was superior to that of PBA-a.

Curing sequence determined the final phase-separated structure, with the mechanism postulated as Scheme 4. In BTA113 [Scheme 4(A)], BA-a reacted first and the intermediate catalyzed the reaction of TBMI. The copolymerization between the two components was so intense that their movements were limited, forming a homogeneous structure. However, TBMI and BA-a reacted sequentially in BTI113 [Scheme 4(B)], without undergoing discernible copolymerization. Thus, when the molecular weight of one component increased to incompatible in thermodynamics, it then moved to form a phase-separated structure.

Table III. Crosslinking Density and Storage Modulus (50°C) of Cured Products based on the DMA Results

Sample	Crosslinking density (10^3 mol m^{-3})	Storage modulus (at 50°C, MPa)
PBA-a	1.49	3280
BTA113	2.63	3439

Influence of Final Structure on Properties

To investigate the influence of final structure on properties, we first calculated the crosslinking density based on DMA results and the rubber elasticity theory following eq. (2),[35] and the corresponding data are summarized in Table III.

$$\rho = E/3\varphi RT \quad (2)$$

Where ρ is the crosslinking density; E is storage modulus in the rubbery region (T_g+40°C); φ is the front factor, which is unity for ideal rubbers; R is the gas constant; and T is the absolute temperature. This equation, which is applicable to polymer networks for lightly crosslinked materials, was herein used only to qualitatively compare the level of crosslinking in the cast resins.[36] The crosslinking densities of BTI113, BTA113, and PBA-a were 2.83 × 10^3 mol m^{-3}, 2.63 × 10^3 mol m^{-3}, and 1.49 × 10^3 mol m^{-3}, respectively, being consistent with T_g values. Meanwhile, the storage moduli (50°C) of cured products are also shown in Table III, following the same tendency as that of T_g.

The toughness properties of cured BTA113 and BTI113 were evaluated by measuring bending deflection and impact strength (Table IV). The bending deflections and impact strengths of cured BTA113 and cured BTI113 exceeded those of PBA-a and PTBMI, meaning that the toughness was improved in blends. Furthermore, the cured BTI113 with bi-continuous structure

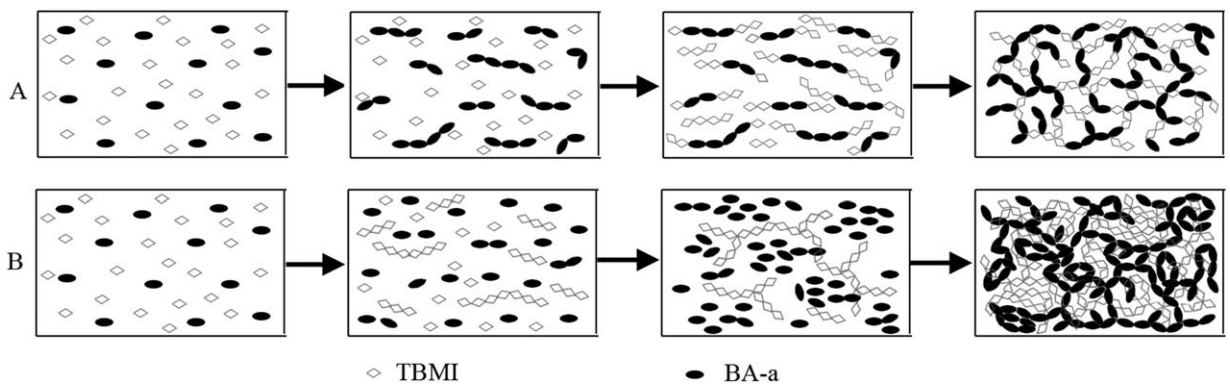

Scheme 4. Proposed mechanism of curing sequence effect on the phase separated structure. BTA113 (A) and BTI113 (B).

Table IV. The Bending Deflection and Impact Strength of Different System

System	PBA-a	PTBMI	BTA113	BTI113
Bending deflection (mm)	4.32	3.17	6.25	6.62
Impact strength (kJ m^{-2})	9.8	7.4	17.1	20.3

had a better toughness property than that of cured BTA113 with homogeneous structure, as evidenced by the higher bending deflection and impact strength.

The augmented toughnesses of BTA113 and BTI113 may be caused by two reasons. First, the blends had higher crosslinking densities than that of PBA-a. Second, the morphology of BTI113 may change the direction of crack propagation and absorb more energy during impact failure. BTI113 had higher impact strength than that of BTA113, which may be ascribed to its morphology because their crosslinking densities were similar.

CONCLUSIONS

The influence of curing sequence of BA-a and TBMI on phase-separated structure was studied by using different catalysts. If BA-a and TBMI reacted sequentially, they were bound to undergo evident copolymerization that limited their movements, forming a homogenous structure. However, if TBMI reacted first, considerable TBMI was consumed at low temperature, so BA-a and TBMI hardly copolymerized, forming a bicontinuous structure instead. Different curing sequences led to different final structures. The crosslinking density and bicontinuous structure positively affected the thermal and toughness properties. When BTA113 and BTI113 had similar crosslinking densities, the morphology was mainly responsible for improving the toughness.

ACKNOWLEDGMENTS

This work is supported by the National Natural Science Foundation of China (Project No.51503187).

REFERENCES

1. Yamanaka, K.; Takagi, Y.; Inoue, T. *Polymer* **1989**, *30*, 1839.
2. Inoue, T. *Prog. Polym. Sci.* **1995**, *20*, 119.
3. Borrajo, J.; Riccardi, C. C.; Williams, R. J. J.; Cao, Z. Q.; Pascault, J. P. *Polymer* **1995**, *36*, 3541.
4. Chen, J. P.; Lee, Y. D. *Polymer* **1995**, *36*, 55.
5. Okada, M.; Fujimoto, K.; Nose, T. *Macromolecules* **1995**, *28*, 1795.
6. Girard-Reydet, E.; Sautereau, H.; Pascault, J. P.; Keatesb, P.; Navardb, P.; Tholletc, G.; Vigier, G. *Polymer* **1998**, *39*, 2269.
7. Tao, Q.; Gan, W.; Yu, Y.; Wang, M.; Tang, X.; Li, S. *Polymer* **2004**, *45*, 3505.
8. Gan, W.; Yu, Y.; Wang, M.; Tao, Q.; Li, S. *Macromol. Rapid Commun.* **2003**, *24*, 952.
9. Kim, B. S.; Inoue, T. *Polymer* **1995**, *36*, 1985.
10. Kim, B. S.; Chiba, T.; Inoue, T. *Polymer* **1995**, *36*, 67.
11. Teng, K. C.; Chang, F. C. *Polymer* **1996**, *37*, 2385.
12. Ratna, D. *Polymer* **2001**, *42*, 4209.
13. Okamoto, Y. *Polym. Eng. Sci.* **1983**, *23*, 222.
14. Girard-Reydet, E.; Sautereau, H.; Pascault, J. P. *Polymer* **1999**, *40*, 1677.
15. Bonnet, A.; Pascault, J. P.; Sautereau, H.; Taha, M.; Camberlin, Y. *Macromolecules* **1999**, *32*, 8517.
16. Fernández-Francos, X.; Foix, D.; Serra, À.; Salla, J. M.; Ramis, X. *React. Funct. Polym.* **2010**, *70*, 798.
17. Santiago, D.; Morell, M.; Fernández-Francos, X.; Serra, À.; Salla, J. M.; Ramis, X. *React. Funct. Polym.* **2011**, *71*, 380.
18. Wang, Z.; Ran, Q.; Zhu, R.; Gu, Y. *RSC Adv.* **2013**, *3*, 1350.
19. Rimdusit, S.; Tiptipakorn, S.; Jubsilp, C.; Takeichi, T. *React. Funct. Polym.* **2013**, *73*, 369.
20. Kwon, Y. H.; Kim, S. C.; Lee, S. Y. *Macromolecules* **2009**, *42*, 5244.
21. He, D.; Cho, S. Y.; Kim, D. W.; Lee, C.; Kang, Y. *Macromolecules* **2012**, *45*, 7931.
22. Narayanan, J.; Jungman, M. J.; Patton, D. L. *React. Funct. Polym.* **2012**, *72*, 799.
23. Wang, Z.; Zhang, Z.; Ran, Q.; Zhu, R.; Gu, Y. *RSC Adv.* **2013**, *3*, 14029.
24. Decker, C.; Nguyen Thi Viet, T.; Decker, D.; Weber-Koehl, E. *Polymer* **2001**, *42*, 5531.
25. Yang, J.; Winnik, M. A.; Ylitalo, D.; DeVoe, R. J. *Macromolecules* **1996**, *29*, 7047.
26. Dean, K. M.; Cook, W. D. *Polym. Int.* **2004**, *53*, 1305.
27. Jannesari, A.; Ghaffarian, S. R.; Molaei, A. *React. Funct. Polym.* **2006**, *66*, 1250.
28. Kimura, H.; Matsumoto, A.; Hasegawa, K.; Ohtsuka, K.; Fukuda, A. *J. Appl. Polym. Sci.* **1998**, *68*, 1903.
29. Pei, D.; Gu, Y.; Cai, X. *Acta Polym. Sin.* **1998**, *1*, 595.
30. White, J. E. *Ind. Eng. Chem. Prod. Res. Dev.* **1986**, *25*, 395.
31. Kissinger, H. E. *Anal. Chem.* **1957**, *29*, 1702.
32. Wang, Z.; Ran, Q.; Zhu, R.; Gu, Y. *J. Appl. Polym. Sci.* **2013**, *129*, 1124.
33. Takeichi, T.; Saito, Y.; Agag, T.; Muto, H.; Kawauchi, T. *Polymer* **2008**, *49*, 1173.
34. Wang, Z.; Zhao, J.; Ran, Q.; Zhu, R.; Gu, Y. *React. Funct. Polym.* **2013**, *73*, 668.
35. Musto, P.; Abbate, M.; Ragosta, G.; Scarinzi, G. *Polymer* **2007**, *48*, 3703.
36. Ishida, H.; Allen, D. J. *Polymer* **1996**, *37*, 4487.